Numerical Analysis of Electrode Geometry Effects on Proton Generation and Acceleration in Pyroelectric Crystal Electrostatic Fields

Shun INOUE[1)], Toru TAKAHASHI[1)], Siyu ZHANG[1)], Toshiki TAKAHASHI[1)]*, Naoki MIZUGUCHI[2)]

[1)] *Graduate School of Science and Technology, Gunma University, 1-5-1 Tenjin-cho, Kiryu, Gunma 376-8515, Japan*
[2)] *National Institute for Fusion Science, National Institutes of Natural Sciences, 322-6 Oroshi-cho, Toki, Gifu 509-5292, Japan*

(Received 16 June 2025 / Accepted 23 June 2025)

To support the development of a compact experimental system for the proton-boron (p-^{11}B) fusion reaction, we performed numerical simulations of proton generation and acceleration in the electrostatic field produced by a pyroelectric crystal. Electrostatic potential distributions were calculated by solving the Laplace equation for three electrode configurations: a disk electrode alone, a disk with a needle electrode, and a disk with a cylinder electrode. The proton impact rate on a boron target placed opposite the electrodes was evaluated for each configuration. It was found that the disk and needle electrodes achieved a maximum impact rate of approximately 37% at a crystal heating temperature of 5 K, while the cylinder electrode achieved a comparable impact rate at a lower temperature of 1 K. These results indicate that the cylinder electrode configuration can achieve efficient proton acceleration at reduced heating temperatures.

Keywords: pyroelectric fusion, proton-boron fusion, beam current, numerical analyses

DOI: 10.1585/pfr.20.1205040

Pyroelectric crystals generate high electric potentials due to changes in their polarization state in response to temperature variations, making them a subject of interest for applications as compact particle accelerators. Pyroelectric X-ray sources have already been commercialized and are utilized in techniques such as X-ray absorption spectroscopy and X-ray fluorescence analysis [1]. When heated, these crystals can accelerate ions. Notably, Naranjo *et al.* were the first to observe deuterium-deuterium (D-D) fusion reactions by accelerating a deuterium beam using a lithium tantalate ($LiTaO_3$) crystal and directing it onto an erbium deuteride (ErD_2) target [2]. Since then, several studies have reported on pyroelectric fusion [3–5], and research continues today, primarily focusing on its application as a compact neutron source [6].

In the field of nuclear fusion, the proton-boron (p-^{11}B) reaction has recently garnered attention due to the relative ease of handling and availability of its fuel. However, the p-^{11}B fusion cross-section is approximately 1.4 barns at an incident proton energy of 675 keV [7], which is significantly lower than the peak value of about 5 barns observed in deuterium-tritium (D-T) fusion at a relative energy of 60–70 keV, indicating that ignition of p-^{11}B fusion is more challenging. For the development of p-^{11}B fusion reactors, small-scale experimental setups that can explore engineering challenges such as reaction environments and energy conversion systems are of great utility. In this context, compact beam accelerators employing pyroelectric crystals are promising candidates. This study conducts numerical simulations of proton acceleration using pyroelectric crystals, aiming to evaluate target impact efficiency for various electrode configurations. The findings are expected to contribute to identifying key challenges in the development of future compact beam accelerator systems.

In this study, the pyroelectric crystal is modeled as a cylinder with a radius of 1 cm and a height of 3 cm, depicted in yellow in Fig. 1. In this study, the “Disk electrode” is regarded as the fundamental geometry of a planar electrode. In previous studies, a needle was mounted at the center of the

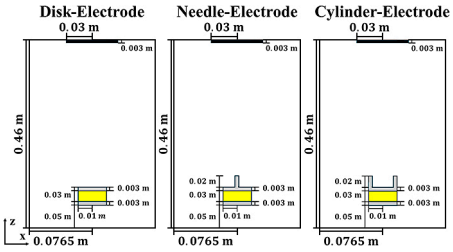

Fig. 1. Schematic cross-sectional views of the experimental setup in the *x*–*z* plane. The left, center, and right panels show configurations with a disk electrode, a disk + needle electrode, and a disk + cylinder electrode, respectively. The yellow region indicates the pyroelectric crystal.

**Corresponding author's e-mail: t-tak@gunma-u.ac.jp*

disk to induce field ionization. To clarify the effect of this configuration, a "Needle electrode" is adopted as the second electrode type. Furthermore, to direct the electric field toward the target, a cylindrical structure was attached to the outer edge of the disk, forming the third electrode type—the "Cylinder electrode". A comparative analysis was conducted among these three electrode configurations. Figure 1 presents a cross-sectional view of the experimental apparatus, illustrating these three distinct electrode geometries. The black region at the top of the apparatus corresponds to a disk-shaped boron target, which serves as the site where accelerated protons strike to initiate the proton-boron (p-^{11}B) fusion reaction.

The electrostatic field generated within the device as a result of heating the pyroelectric crystal is computed by solving the Laplace equation. The outer boundary of the device, as shown in Fig. 1 (outlined by the black lines in all three subfigures), is a grounded metallic enclosure. The internal, axisymmetric region is represented using a cylindrical coordinate system (in the two-dimensional r–z plane). The computational domain is discretized using a uniform grid, with 256 divisions in both the r and z directions.

The maximum electric potential, $\phi_{\max}$, on the electrode surface is determined using Gauss's law near the electrode, expressed as:

$$E_z = -\frac{\phi_{\max}}{z_d}\frac{\partial\bar{\phi}}{\partial\bar{z}} = \frac{\gamma\Delta T}{\varepsilon_0}, \text{ where } \bar{\phi} \equiv \frac{\phi}{\phi_{\max}},\ \bar{z} \equiv \frac{z}{z_d}.$$

Here, $\phi_{\max}$ [V] can be calculated since the normalized potential gradient $\partial\bar{\phi}/\partial\bar{z}$ is obtained from the numerical solution of the Laplace equation. In this expression, γ denotes the pyroelectric coefficient, which is 190 μC/(m^2·K) for lithium tantalite [3]. ΔT [K] is the temperature change in the pyroelectric crystal, and z_d is the device length, taken to be 0.46 m.

A color contour of the calculated potential distribution is presented in Fig. 2. In all three cases, the maximum potential is approximately $\phi_{\max} \sim 237\Delta T$ [kV], and the potential distribution in the figure is normalized by $\phi_{\max}$. The electric field is concentrated near the electrode in all cases, with the cylinder electrode exhibiting a high-potential region extending into the cylinder.

The electrostatic field depicted in Fig. 2 serves to accelerate electrons. As the heating of the pyroelectric crystal progresses, relativistic effects become significant in the electron dynamics. Consequently, the relativistic equation of motion is numerically integrated to simulate the electron motion. At time t = 0, the electrons are assumed to be uniformly distributed in space. Accelerated electrons subsequently collide with hydrogen atoms, leading to proton production. The ionization of hydrogen by electron impact is modeled using pseudorandom numbers, as described in [8].

As an example, the positions of proton generation are projected onto the x–z plane using the Disk electrode and are indicated as black dots in Fig. 3. The ionization cross-section of hydrogen due to electron impact is relatively large in the energy range of several tens of eV to 100 eV, but it decreases significantly above 100 eV, resulting in reduced ionization of hydrogen. Therefore, as the heating temperature increases, ionization collisions become less frequent in the region of the concentrated electric field near the electrode, leading to a decreased likelihood of proton generation. At a heating temperature of 100 K, proton generation becomes negligible. Moreover, even when protons are produced, they are excessively accelerated, far exceeding the energy of 675 keV at which the cross-section for the p-^{11}B reaction peaks. As a result, these protons do not significantly contribute to nuclear reactions. This highlights the necessity of moderate heating to optimize reaction efficiency.

Figure 4 shows the relationship between the crystal heating temperature and the proton impact rate on the boron target. As illustrated in Fig. 1, the boron target is a disk-shaped structure with a radius of 3 cm and a thickness of 3 mm. The proton impact rate is defined as the fraction of generated protons that collide with the boron target. In the cases of the disk and needle electrodes, the highest impact rate—approximately 37%—is achieved at a heating temperature of 5 K. In contrast, the cylinder electrode exhibits a different trend: a comparable impact rate is attained with only 1 K of heating.

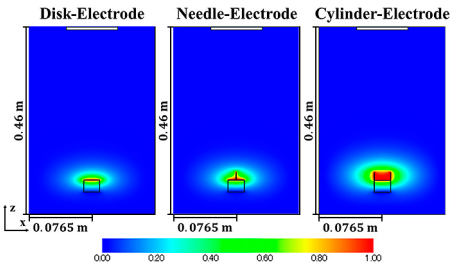

Fig. 2. Color contour plots of the normalized electric potential $\phi/\phi_{\max}$ in the x–z plane. The arrangement of the panels is the same as in Fig. 1.

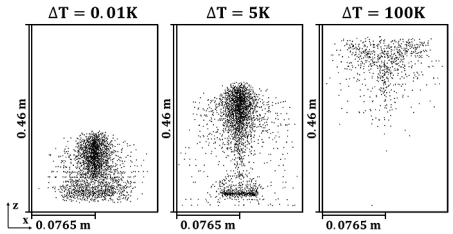

Fig. 3. Proton generation locations near the needle electrode. The left, center, and right panels correspond to crystal heating temperatures of ΔT = 0.01, 5, and 100 K, respectively.

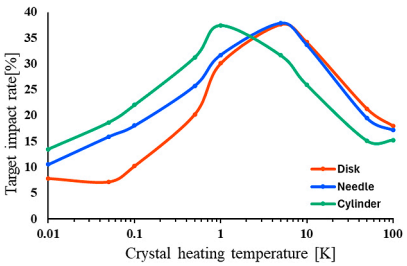

Fig. 4. Dependence of proton impact rate on the target as a function of crystal heating temperature for the three electrode configurations.

This work was performed with the support and under the auspices of the NIFS Collaboration Research program (NIFS24KISC009 and NIFS24KIPC003).

[1] J. Kawai *et al.*, X-Ray Spectrom. **41**, 216 (2012).
[2] B. Naranjo *et al.*, Nature **434**, 1115 (2005).
[3] J. Geuther *et al.*, Phys. Rev. Lett. **96**, 054803 (2006).
[4] D. Gillich *et al.*, Nucl. Instrum. Methods Phys. Res. A **602**, 306 (2009).
[5] M.M. Nasseri, Nucl. Instrum. Methods Phys. Res. B **362**, 45 (2015).
[6] S. Mohtashami *et al.*, J. Appl. Phys. **135**, 200701 (2024).
[7] S.H. Sikora *et al.*, J. Fusion Energy **35**, 538 (2016).
[8] T. Takahashi *et al.*, Phys. Plasmas **11**, 3131 (2004).